

Dual-Emission Single Sensing Element-Assembled Fluorescent Sensor Array for the Rapid Discrimination of Multiple Surfactants in Environments

Dali Wei¹, Hu Zhang¹, Yu Tao¹, Kaixuan Wang¹, Ying Wang¹, Chunmeng Deng¹, Rongfei Xu¹, Nuanfei Zhu¹, Yanyan Lu¹, Kun Zeng¹, Zhugen Yang², Zhen Zhang^{1}*

¹School of Emergency Management, School of the Environment and Safety Engineering, Jiangsu University, Zhenjiang 212013, China.

²School of Water, Energy, and Environment, Cranfield University, Milton Keynes, MK43 0AL, UK

*Corresponding author:

Email: zhangzhen@ujs.edu.cn.

ABSTRACT

Surfactants are considered as typical emerging pollutants, and extensive use of which in disinfectants brings huge threat to ecosystem and human health, particularly during the pandemic of coronavirus disease-19 (COVID-19), whereas the rapid discrimination of multiple surfactants in environments is still a great challenge. Herein, we designed a fluorescent sensor array based on luminescent metal-organic frameworks (UiO-66-NH₂@Au NCs) for the specific discrimination of six surfactants (AOS, SDS, SDSO, MES, SDBS, and Tween-20). Wherein, UiO-66-NH₂@Au NCs was fabricated by integrating UiO-66-NH₂ (2-aminoterephthalic acid - anchored-MOFs based on zirconium ions) with gold nanoclusters (Au NCs), which exhibited a dual-emission features, showing good luminescence. Interestingly, due to the interactions of surfactants and UiO-66-NH₂@Au NCs, the surfactants can differentially regulate the fluorescence property of UiO-66-NH₂@Au NCs, producing diverse fluorescent “fingerprints”, which were further identified by pattern recognition methods. The proposed fluorescence sensor array achieved 100% accuracy in identifying various surfactants and multi-component mixtures, with the detection limit in the range of 0.0032 to 0.0315 mM for six pollutants, which was successfully employed in the discrimination of surfactants in real environmental waters. More importantly, our finding provided a new avenue in rapid detection of surfactants, rendering a promising technique for environmental monitoring against trace multi-contaminants.

Keywords: emerging pollutants, rapid detection, metal-organic frameworks, surfactants, sensor array

INTRODUCTION

Under the background of coexistence of coronavirus disease-19 (COVID-19) and human beings, surfactants are usually added into disinfectants to provide a synergistic effect with alcohols to inactivate the coronavirus.¹⁻⁴ However, extensive use of disinfectants usually leads to the release of surfactants into the ecosystem, resulting in a series of environmental issues. In addition, exposure to surfactants with high concentrations can cause adverse health effects, such as irritation to human eyes and skin.⁴⁻⁶ In recent years, environmental health problems caused by surfactants have received extensive attentions.⁷⁻⁹ To date, many instrumental methods for surfactants detection have been developed,^{8, 10} but these techniques were hampered in wide applications due to high cost, tedious procedures, and time-consuming analysis.¹¹⁻¹² Thus, it is essential to explore simple, efficient, and high-throughput methods to detect environmental surfactants for risk assessment.

Inspired by the olfactory or gustatory system, sensor array has become a powerful tool in biosensing, especially in rapid discrimination of multiple targets in complex samples.¹³⁻¹⁶ Typically, the identification of various analytes can be realized by analyzing the characteristic fingerprints originated from the responses of probes to analytes.^{15, 17-19} Nevertheless, the development of sensor array for surfactant identification is rarely reported.²⁰⁻²¹ Wherein, Luo et al. synthesized two fluorescent nanomaterials as signal receptors to establish a fluorescent sensor array for multiple surfactants detection,²⁰ whereas the preparation of multiple sensing units will increase the synthetic cost, analytical operation, and detection time,²² as well as disturb the repeatability.²³⁻²⁴ To simplify the array, an individual sensing unit with multiple signal channels could provide an effective strategy to avoid the above issues,^{22, 25} highlighting the variations between individual analyte based on the completely different responses.²⁶ For instance, Yu et al. prepared an Au-Ag nanocomposite with three signal channels (the fluorescence, light scattering and absorption) as sensing units against sulfur species.²⁷ However, various output signals still required additional instruments and measurements.^{22, 25} As an alternative, it is important to design a sensor array based on single sensing unit with multiple response channels for multi-surfactants detection, especially for a single measurement.

Herein, we prepared a luminescent metal-organic framework (UiO-66-NH₂@Au NCs) with

two response channels by integrating UiO-66-NH₂ with Au NCs for constructing an array sensor for the rapid and high-throughput discrimination of six surfactants (AOS, SDS, SDSO, SDBS, MES, and Tween-20) (**Scheme 1**). Owing to the various responses between surfactants and UiO-66-NH₂@Au NCs, the “fingerprints” generated from the fluorescence signals were further analyzed by pattern recognition methods for surfactant identification. Under conditions optimization, the proposed fluorescence sensor array achieved sensitive measurement for the six surfactants, which also indicated good performance in the distinction of surfactants and their mixtures in the actual samples. This strategy based on multiple channels originating from a single material was shown to be low-cost, simple to operate and easy to test, which not only bridged the gap of existing rapid detection methods of surfactants, but also opened a new way for environmental monitoring.

MATERIALS AND METHODS

Synthesis of UiO-66-NH₂

The preparation of UiO-66-NH₂ was relied on the previous studies.^{20, 28} In brief, ZrCl₄ (0.129 mM, 30 mg), BDC-NH₂ (0.110 mM, 20 mg), and benzoic acid (4.918 mM, 600 mg) in 2 mL of DMF were ultrasonically dissolved, and transferred into reactor. The mixture was heated in an oven at 120 °C for 12 h. After reaction, the resultants were collected and washed with DMF and acetone to remove unreacted precursors. The resulting UiO-66-NH₂ was dried at 60 °C and stored at room temperature.

Preparation of UiO-66-NH₂@Au NCs

The synthesis of UiO-66-NH₂@Au NCs was based on the in-situ induction of Au NCs on UiO-66-NH₂.²⁹⁻³² Typically, UiO-66-NH₂ (10 mg) was dissolved into 13.6 mL of water by sonication, and then 6 mL of GSH (3 mg/mL) solution was added and stirred thoroughly for 15 min. Next, 0.4 mL HAuCl₄ (60 mM) was added into the above mixture under vigorous stirring for 10 min, the above solution was heated to 70 °C under gentle stirring for 24 h. The resultants were collected and washed with water for three times, and dried in an oven at 60 °C.

Fluorescence Sensor Array for the Discrimination of Surfactants.

The sensor array was composed of UiO-66-NH₂@Au NCs with dual-emission, six surfactants (AOS, SDS, SDSO, SDBS, MES, and Tween-20), and five replicates. Briefly, six

surfactants and blank sample as a control were mixed with UiO-66-NH₂@Au NCs respectively, and the mixtures were incubated at 25 °C for 4 min. Then, the fluorescence intensity of the mixtures at 450 and 614 nm were recorded by a fluorescence spectrometer. Consequently, six surfactants were measured against the UiO-66-NH₂@Au NCs five times to provide a training-data matrix of 2 channels×6 surfactants×5 replicates. The obtained data were normalized and analyzed by linear discriminant analysis (LDA) and hierarchical cluster analysis (HCA) for the differentiation of six surfactants.

Identification of Surfactants in Actual Samples.

The practicability of the fluorescent sensor array in actual samples was assessed. Firstly, six surfactants (AOS, SDS, SDSO, SDBS, MES, and Tween-20) were added into the tap water samples, and then the above mixtures were detected by the proposed fluorescent sensor array. The fluorescence intensity was recorded by a fluorescence spectrometer, and the recovery rate of six surfactants in tap water were calculated. Meanwhile, unknown samples containing different surfactants at various concentrations were tested by the proposed sensor array with a double-blind protocol. In addition, to further study the feasibility of the fluorescent sensor array in actual samples, 11 kinds of washing and disinfecting products were collected in local markets, including hand sanitizer, disinfectant, and detergent etc., which were also detected by the proposed sensor array.

RESULTS AND DISCUSSION

Characterization of UiO-66-NH₂@Au NCs.

Figure 1a demonstrated the synthetic strategy of UiO-66-NH₂@Au NCs by in-situ synthesis of Au NCs on UiO-66-NH₂. Characterized by TEM images, pure UiO-66-NH₂ presented typical octahedral morphology (**Figure 1b**), and the average size was about 250 nm. As shown in **Figure 1c**, the Au NCs with spherical structure presented a good dispersibility, and their average size was about 1.74 nm (**Figure S1**). The prepared pure UiO-66-NH₂ and Au NCs were similar to previous studies.^{29, 33-35} After integrating UiO-66-NH₂ and Au NCs, a luminescent metal-organic framework (UiO-66-NH₂@Au NCs) was obtained, which still showed a regular octahedral structure (**Figure 1d**), indicating that the modification of Au NCs had no significant effects on the crystallinity of UiO-66-NH₂. As presented in HRTEM images of individual UiO-

66-NH₂@Au NCs (**Figure 1e**), there were some black dots (Au NCs) on the surface of UiO-66-NH₂, and the lattice spacing of Au NCs were obviously observed, implying that the successful modification of Au NCs on UiO-66-NH₂. In addition, elemental mapping in HAADF-STEM image demonstrated that the elements (C, N, O, Zr, and Au) could be observed in individual UiO-66-NH₂@Au NCs, wherein Au was evenly distributed on the surface of UiO-66-NH₂, implying the preparation of UiO-66-NH₂@Au NCs nanocomposites (**Figure 1f**).

The features of the synthesized UiO-66-NH₂@Au NCs was further assessed. As depicted in **Figure 2a**, the PXRD patterns of UiO-66-NH₂@Au NCs was consistent with the pure UiO-66-NH₂ and the simulated one, demonstrating that the modification of Au NCs had no effects on the crystallinity of UiO-66-NH₂. Meanwhile, absorption spectrum of UiO-66-NH₂@Au NCs presented that the absorption peak at 240 nm shifted to 250 nm after fabricating with Au NCs on UiO-66-NH₂ (**Figure 2b**). In addition, a comparison of the UiO-66-NH₂@Au NCs and UiO-66-NH₂ was studied by the FT-IR spectrometer (**Figure 2c**). Wherein, the characteristic peaks at 3460, 1250, and 760 cm⁻¹ were assigned to the stretching vibration of amino groups, the N-H wagging band and the strong C-N stretching band,^{20, 31} respectively, and the peak at 1570 cm⁻¹ was the stretching vibration of the carboxyl group coordinated with Zr⁴⁺ in FT-IR analysis of UiO-66-NH₂.^{31, 33} Meanwhile, similar typical peaks were observed in UiO-66-NH₂@Au NCs, demonstrating the successful fabrication of UiO-66-NH₂@Au NCs.³⁶⁻³⁷ Besides, the chemical compositions of UiO-66-NH₂@Au NCs were verified by XPS spectrum. The peaks of O 1s, N 1s, C 1s, Zr 3d, S 2p, and Au 4f all appeared in the survey spectrum (**Figure 2d**), suggesting the preparation of UiO-66-NH₂@Au NCs. Wherein, two peaks at 182.9 and 185.2 eV in Zr 3d spectrum were attributed to the binding energies for Zr 3d_{5/2} and Zr 3d_{3/2}, which was related to the ligand BDC-NH₂ (**Figure 2e**).^{20, 38} Meanwhile, three peaks at 530.2, 531.4, and 532.7 eV in O 1s spectrum were originated from the binding energies of Zr-O-Zr, Zr-OH, and -OH,^{20, 39} respectively (**Figure S2**). In addition, two peaks at 83.48 and 87.18 eV, were ascribed to the binding energies for Au 4f_{7/2} and Au 4f_{5/2}, suggesting the fabrication of Au NCs on UiO-66-NH₂ (**Figure 2f**). Moreover, the contents of each element in UiO-66-NH₂@Au NCs were shown in **Table S1**. The results showed that the proportion of C and O elements were 67.25% and 18.46%, respectively, which were attributed to that UiO-66-NH₂@Au NCs possessing C-C and C=O bonds. Besides, the proportion of Au and S elements were similar

(2.84% and 2.49%), indicating that the UiO-66-NH₂@Au NCs contained abundant gold nanoclusters. These results revealed the successful fabrication of UiO-66-NH₂@Au NCs.

Luminescent Property of UiO-66-NH₂@Au NCs.

The fluorescence properties of UiO-66-NH₂@Au NCs was assessed. As described in **Figure 2g**, the characteristic emission peaks of UiO-66-NH₂ and Au NCs were at 450 nm and 650 nm, respectively.^{30,40} And the luminescent MOFs (UiO-66-NH₂@Au NCs) exhibited dual-emission properties, and the characteristic emission peaks were at 450 and 614 nm. Wherein, the fluorescent peak at 450 nm was derived from UiO-66-NH₂, whereas the emission peak of Au NCs shifted from 650 nm to 614 nm after the fabrication of Au NCs on the UiO-66-NH₂.³¹ These results suggested that UiO-66-NH₂@Au NCs exhibited a two-channels fluorescent signal, indicating the successful fabrication of single sensing unit with multiple response channels. Characterized by CIE chromaticity diagram (**Figure 2h**), the CIE coordinate of the band at 450 nm of UiO-66-NH₂ and at 614 nm of Au NCs were calculated to be (0.137, 0.101) and (0.585, 0.414). After the combination of UiO-66-NH₂ and Au NCs, the CIE coordinate of the UiO-66-NH₂@Au NCs (0.350, 0.305) was situated the coordinate for a saturated white emitter.²⁵ And the photographs of UiO-66-NH₂, Au NCs, and UiO-66-NH₂@Au NCs solution under UV lamp irradiation were consistent with the results of CIE coordinate (**Figure 2i**). Then, the fluorescence lifetime of UiO-66-NH₂@Au NCs was measured, and the results showed that the average fluorescence lifetimes at 450 and 614 nm were 7.02 and 8.02 ns, respectively (**Figure S3** and **Table S2**), suggesting the good fluorescence property of UiO-66-NH₂@Au NCs. Besides, the stability results presented that the synthesized UiO-66-NH₂@Au NCs could maintain good fluorescence properties under UV irradiation, long storage, and different pH (**Figure S4**).⁴¹

Fluorescence Sensor Array for the Differentiation of Surfactants.

Owing to the diverse fluorescence responses of six surfactants to dual-emission profiles of the UiO-66-NH₂@Au NCs, the single luminescent metal-organic framework was employed to design a fluorescent sensor array for the differentiation of six surfactants, including AOS, SDS, SDO, SDBS, MES, and Tween-20 (**Figure 3a**). Shown in **Figure 3b**, when the UiO-66-NH₂@Au NCs was mixed with different surfactants, the fluorescence intensities of UiO-66-NH₂@Au NCs at 450 and 614 nm appeared apparent and various responses. Wherein, AOS,

SDSO, and SDBS could remarkably improve the fluorescence intensity at 450 nm of UiO-66-NH₂@Au NCs, whereas a “turn-off” response at 614 nm was observed after adding AOS, SDS, SDSO, MES, and Tween-20. Then, the obtained fluorescence intensities were collected for producing pattern F/F_0 data, and results showed the generation of various fluorescence responses of UiO-66-NH₂@Au NCs to different surfactants (**Figure 3c**), which could be analyzed by pattern recognition methods for the recognition of six surfactants. In addition, the corresponding heat map suggested the diverse fluorescence responses of UiO-66-NH₂@Au NCs to six surfactants (**Figure 3d**). By introducing the linear discriminant analysis (LDA), the training matrix (1 arrays×6 surfactants×5 replicates) generated from fluorescence responses patterns (F/F_0 data) were converted into “fingerprints” and produced two Factors. Wherein, the two factors (factor 1, 91.77%; factor 2, 8.23%) were employed to create a two-dimensional (2D) plot, and the six surfactants were accessible to be separated from each other without overlap, suggesting that the fluorescence responses derived from proposed sensor array could be used for the distinction of six surfactants by the LDA (**Figure 3e**). Meanwhile, hierarchical cluster analysis (HCA) was employed to evaluate the comparability of six surfactants.⁴² As shown in **Figure 3f**, all of the 30 cases (6 surfactants×5 replicates) were correctly distributed to their respective groups with no misclassification or error. On this basis, the identification capability of sensor array was further assessed by analyzing these surfactants at various concentrations (1, 0.1, and 0.01 mM), which presented good fluorescence response fingerprints, and achieved an overall accuracy of 100.0% for the fingerprint of different concentration of surfactants (**Figure S5**).⁴³ The above results of LDA and HCA indicated that the obtained sensor array platform can achieve a rapid and effective identification for surfactants, with good accuracies and feasibilities.

Mechanism of Fluorescence Sensor Array for Surfactants Detection.

In this study, the mechanism of fluorescence sensor array for surfactants detection was further discussed, and the structure differences of these surfactants could induce different interactions between surfactants and UiO-66-NH₂@Au NCs, resulting in various fluorescence responses (**Figure S6**). Firstly, the influences of surfactants on the morphology of UiO-66-NH₂@Au NCs was investigated, and the results in **Figure S7** revealed that UiO-66-NH₂@Au NCs still maintained an octahedral structure with the addition of the surfactants. In addition,

the PXRD results also presented that the participation of surfactants showed no obvious effects on the structure of the UiO-66-NH₂@Au NCs (**Figure S8**). The above results suggested that the fluorescence responses were not attributed to the morphology change of UiO-66-NH₂@Au NCs. Then, the fluorescence lifetimes of the mixture of UiO-66-NH₂@Au NCs and surfactants were further evaluated. In this study, AOS and SDSO could enhance fluorescence intensity of UiO-66-NH₂@Au NCs at 450 nm, whereas other surfactants showed the quenching effect on the fluorescence intensity at 614 nm. Thus, AOS, SDSO, and Tween-20 were employed as typical surfactants for monitoring the fluorescence lifetime. As shown in **Figure S9**, the addition of AOS and SDSO could prolong the fluorescence lifetime of UiO-66-NH₂@Au NCs at 450 nm, thereby enhancing the fluorescence intensity, and significantly decrease the fluorescence lifetime at 614 nm, resulting in fluorescence quenching (**Table S2**). As a nonionic surfactant, Tween-20 exhibited different responses from anionic surfactants (AOS, SDSO), and significantly reduced the fluorescence lifetime of UiO-66-NH₂@Au NCs at 450 and 614 nm, indicating that the decrease of fluorescence lifetime was the main factor of fluorescence quenching. According to the previous studies, when the value of τ_0/τ was similar to the value of F_0/F , the quenching principle could be regarded as dynamic quenching. By contrast, the value of τ_0/τ was 1, the quenching mechanism could be considered as static quenching.^{20, 43-45} In this study, the response between UiO-66-NH₂@Au NCs and SDSO was chose as an example to investigate the quenching mechanism. Shown in **Table S2**, the τ_0 and τ value of UiO-66-NH₂@Au NCs at 614 nm was 8.05 and 6.61 ns, respectively, and the value of τ_0/τ was 1.22, which was close to the value of F_0/F (1.31), implying that the quenching response was caused by dynamic association.

Fluorescence Sensor Array for the Quantitative Determination of Surfactants.

The proposed sensor array could accomplish the qualitative discrimination of six surfactants by the pattern recognition methods. To achieve satisfactory discriminations of the six surfactants, the optimal conditions of the fluorescence sensor array was further studied, including incubation time, probe concentration, and pH. As shown in **Figure S10-12**, 4 min, 1.54 mg/mL, and pH=7 was selected as the optimal parameter conditions for the quantitative discrimination of six surfactants, respectively. Wherein, the fluorescence responses of the array sensor to varying concentrations of AOS and SDBS were collected as examples for testifying

quantitative detection. In the canonical score plot (**Figure 4a-c**), AOS with different concentrations (0.015-0.5 mM) could be efficiently distinguished, and a good linear relationship between the fluorescence intensity of UiO-66-NH₂@Au NCs and AOS was obtained. As shown in **Table S3**, the limit of detection (LOD) for AOS was calculated to be 0.0032 mM. Meanwhile, the quantitative detection for SDBS by the proposed sensor array was established, and the limit of detection (LOD) for SDBS was 0.023 mM (**Figure 4d-f**). In addition, other surfactants (SDS, SDSO, MES, and Tween-20) with different concentrations could be efficiently differentiated (**Figure S13**), and the LOD of the fluorescence sensor array for SDS, SDSO, MES, and Tween-20 detection were 0.0311, 0.0315, 0.03, and 0.028 mM, respectively (**Table S3**).

To testify the discrimination ability of the surfactant mixtures, the binary and ternary mixtures were measured by the proposed sensor array. First, the compound of SDSO and MES with varying molar ratios were prepared (SDSO 100%, SDSO 80%+MES 20%, SDSO 60%+MES 40%, SDSO 50%+MES 50%, SDSO 40%+MES 60%, SDSO 20%+MES 80%, and MES 100%), which was further evaluated by the fluorescent sensor array. And the fluorescent responses of UiO-66-NH₂@Au NCs for the binary mixtures of SDSO and MES were collected and analyzed by the LDA and HCA. As showed in **Figure 4g and S14a**, individual SDSO, MES, and binary mixtures were accurately identified against one another with no error or misclassifications. Meanwhile, ternary mixtures containing SDSO, MES, and SDBS were employed as examples to verified, which also presented good identification capacity (**Figure 4h and S14b**). In addition, for the fingerprint of individual surfactant, binary and ternary mixtures of surfactants, it achieved an overall accuracy of 100.0% (**Figure 4i**). In addition, the anti-interference ability of the proposed sensor array was also investigated, and the multiple typical cations (Na⁺, K⁺, Mg²⁺, Zn²⁺, Fe²⁺, and Ca²⁺) and anions (CO₃²⁻, SO₄²⁻, and Cl⁻) were added into the sensor array for the identification of surfactants. As depicted in **Figure S15**, the complete separation of all interfering ions from the six groups of surfactants, indicating the superior interference capacity of the sensor arrays. These results proved the good performance of the proposed fluorescence sensor array based on UiO-66-NH₂@Au NCs for the identification of surfactant mixtures, laying a good foundation for the detection of surfactants in actual samples.

Identification of Surfactants in Real Samples.

To validate the ability of the proposed sensor array in identifying multiple surfactants, unknown samples containing different surfactants at various concentrations were tested with a double-blind protocol. Among 30 samples, 28 of them are correctly identified by the fluorescence sensor array, providing identification accuracy of 93.33% (**Table S4**). The results verified the great potentials of the fabricated sensor array in identifying and distinguishing multiple surfactants. Wherein, tap water samples were spiked into 6 different surfactants at the concentration of 0.1 mM, after which their fluorescence responses were measured. The LDA and PCA results displayed that the selected surfactants were well separated from each other with good accuracy (**Figure 5a and 5b**), and the recoveries of 6 surfactants ranged from 96.9 to 103.3% (**Table S5**). In addition, the measured value by the proposed fluorescent sensor array could well correspond with the measured value obtained from the LC-MS/MS method, indicating the good precision and accuracy of our established sensor array. In addition, the ability of recognizing the surfactants mixtures in real samples was further verified. Wherein, three mixed groups (AOS: SDS=1:1; SDS: Tween-20=1:1; AOS: SDS: Tween-20=1:1:1) were added to the water samples, which were further assessed by the established sensor array. As shown in **Figure 5c and 5d**, the LDA and PCA results showed that the surfactants mixtures were well separated with 100% accuracy, demonstrating the utility of the established sensor array for distinction of mixed surfactants in real samples.

To further verify the practical application of the proposed sensor array, 11 kinds of washing and disinfecting products were collected in local market, including hand sanitizer, sanitizer gel, disinfectant, and disinfectant wipes, etc., which were detected by the proposed sensor array. As shown in **Figure 5e**, some surfactants were found in the collected sanitizer gel and disinfectant, and other real samples (hand sanitizer, 84 disinfectants, and antiseptic wipes) did not detect any surfactants, which were presented in **Table S6**. However, it was difficult to achieve the quantitative analysis of these surfactants in real samples due to the complexity of the collected sample, and the compositions were not as ideal as water samples used in experiments. Fortunately, a fluorescence sensor array will be combined with artificial intelligence and deep learning based on the numerous training data and appropriate processing algorithms in the future for achieving the identification of surfactants residues in real samples.

CONCLUSIONS

In this study, a single sensing element-assembled fluorescent sensor array with dual-emission property was proposed for the rapid identification of multiple surfactants in environments. The structural differences of six surfactants endowed their various interactions with the UiO-66-NH₂@Au NCs, resulting in diverse fluorescence responses, which were collected and analyzed by combining HCA and LDA for the identification of six surfactants with high selectivity and sensitivity. Meanwhile, the fabricated fluorescence sensor array showed good performance in the identification of various surfactants and their mixtures, which were successfully employed for detecting surfactants in actual water samples. This sensor array based on single sensing probe with multiple channels exhibited the advantages of low-cost, simple to operate, and easy to test, which bridged the gap of rapid detection of surfactants, opening a new way for the identifications of multiple emerging contaminants in environments.

ASSOCIATED CONTENT

Supporting Information

Characterization of Au NCs; fluorescence lifetime and stability of UiO-66-NH₂@Au NCs; assessment of the sensor array for six surfactants at different concentrations; chemical structures of six surfactants; TEM images and PXRD patterns of UiO-66-NH₂@Au NCs with different surfactants; fluorescence lifetime of UiO-66-NH₂@Au NCs with AOS, SDSO, and Tween-20; optimal conditions of the sensor array for surfactants detection; quantitative determination of Tween-20, MES, SDBS, and SDS; evaluation of the sensor array for binary and ternary mixtures; elemental quantification by XPS for UiO-66-NH₂@Au NCs; the recovery of six surfactants in real samples by the proposed sensor array (PDF).

Notes

The authors declare no competing financial interest.

ACKNOWLEDGMENTS

This work was supported by the National Natural Science Foundation of China (Grants No. 21876067, 22176075), the special scientific research project of School of Emergency Management, Jiangsu University (KY-D-17), the personnel training project of School of

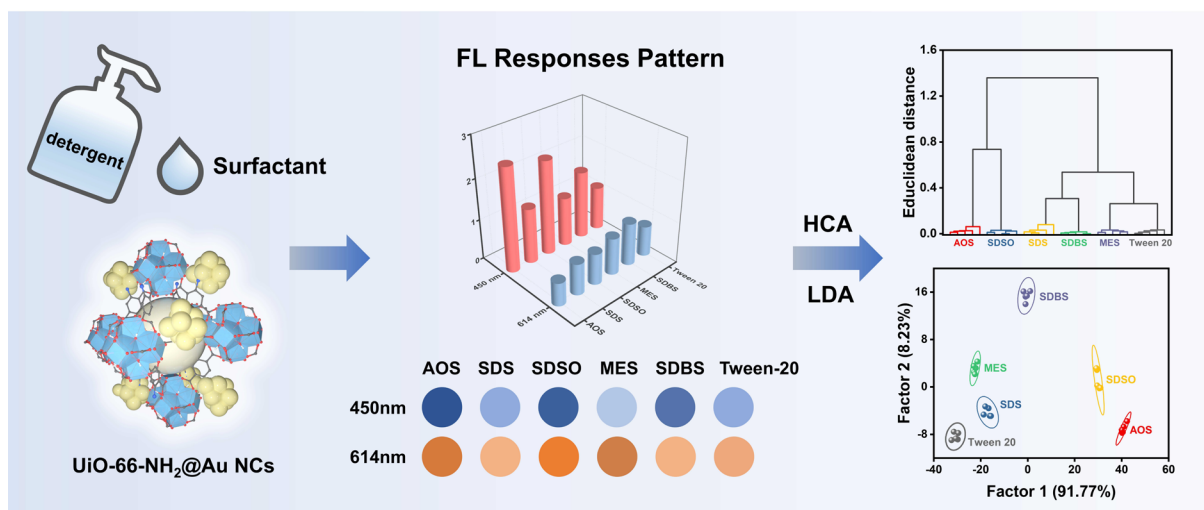
Emergency Management, Jiangsu University (JG-03-13), and the Jiangsu Collaborative Innovation Center of Technology and Material of Water Treatment.

REFERENCES

- (1) Jahromi, R.; Mogharab, V.; Jahromi, H.; Avazpour, A., Synergistic effects of anionic surfactants on coronavirus (SARS-CoV-2) virucidal efficiency of sanitizing fluids to fight COVID-19. *Food Chem Toxicol* **2020**, *145*, 111702.
- (2) Das, B.; Kumar, B.; Begum, W.; Bhattarai, A.; Mondal, M. H.; Saha, B., Comprehensive Review on Applications of Surfactants in Vaccine Formulation, Therapeutic and Cosmetic Pharmacy and Prevention of Pulmonary Failure due to COVID-19. *Chem Afr* **2022**, *5* (3), 459-480.
- (3) Hu, S.; Fang, S.; Zhao, J.; Wang, G.; Qi, W.; Zhang, G.; Huang, C.; Qu, J.; Liu, H., Toxicity Evaluation and Effect-Based Identification of Chlorine Disinfection Products of the Anti-COVID-19 Drug Chloroquine Phosphate. *Environ Sci Technol* **2023**, *57* (21), 7913-7923.
- (4) Zhou, P.; Kong, Y.; Cui, X., Inhalation Bioaccessibility of Polycyclic Aromatic Hydrocarbons in PM_{2.5} under Various Lung Environments: Implications for Air Pollution Control during Coronavirus Disease-19 Outbreak. *Environ Sci Technol* **2022**, *56* (7), 4272-4281.
- (5) Lechuga, M.; Fernández-Serrano, M.; Jurado, E.; Núñez-Olea, J.; Ríos, F., Acute toxicity of anionic and non-ionic surfactants to aquatic organisms. *Ecotoxicol Environ Saf* **2016**, *125*, 1-8.
- (6) Mustapha, D. S.; Bawa-Allah, K. A., Differential toxicities of anionic and nonionic surfactants in fish. *Environ Sci Pollut R* **2020**, *27* (14), 16754-16762.
- (7) Badmus, S. O.; Amusa, H. K.; Oyehan, T. A.; Saleh, T. A., Environmental risks and toxicity of surfactants: overview of analysis, assessment, and remediation techniques. *Environ Sci Pollut R* **2021**, *28* (44), 62085-62104.
- (8) Huang, Y.; Shen, Y.; Li, S.; Zheng, R.; Zhang, C.; Li, B.; Zhang, K., Dual-emission samarium macrocycle as a lab-on-a-molecule enables high-throughput discrimination of anionic sulfonate surfactants. *Sensor Actuat B-Chem* **2021**, *348*, 130679.
- (9) Lee, S.; Lee, K. M.; Lee, M.; Yoon, J., Polydiacetylenes Bearing Boronic Acid Groups as Colorimetric and Fluorescence Sensors for Cationic Surfactants. *ACS Appl Mater Interfaces* **2013**, *5* (11), 4521-4526.
- (10) Wiest, L.; Giroud, B.; Assoumani, A.; Lestremau, F.; Vulliet, E., A multi-family offline SPE LC-MS/MS analytical method for anionic, cationic and non-ionic surfactants quantification in surface water. *Talanta* **2021**, *232*, 122441.
- (11) Niu, X.-X.; Xu, Q.-C.; Li, A.-Z.; Li, Y.-J.; Zhang, X.-T.; Zhang, Y.; Xing, G.-W., A BODIPY-carbazole hybrid as a fluorescent probe: the design, synthesis, and discrimination of surfactants and the determination of the CMC values. *Analyst* **2019**, *144* (23), 6866-6870.
- (12) Wei, D.; Li, M.; Ai, F.; Wang, K.; Zhu, N.; Wang, Y.; Yin, D.; Zhang, Z., Fabrication of Biomimetic Cascade Nanoreactor Based on Covalent Organic Framework Capsule for Biosensing. *Anal Chem* **2023**, *95* (29), 11052-11060.
- (13) Meng, H.; Wang, Y.; Wu, R.; Li, Y.; Wei, D.; Li, M.; Zhu, N.; Zhu, F.; Zhang, Z.; Zhao, H., Identification of multi-component metal ion mixtures in complex systems using fluorescence sensor arrays. *J. Hazard. Mater.* **2023**, *455*, 131546.
- (14) Chen, Z.-H.; Fan, Q.-X.; Han, X.-Y.; Shi, G.; Zhang, M., Design of smart chemical 'tongue' sensor arrays for pattern-recognition-based biochemical sensing applications. *Trends Anal. Chem.* **2020**, *124*, 115794.

- (15) Li, T.; Zhu, X.; Hai, X.; Bi, S.; Zhang, X., Recent Progress in Sensor Arrays: From Construction Principles of Sensing Elements to Applications. *ACS Sens* **2023**, *8* (3), 994-1016.
- (16) Yang, M.; Zhang, M.; Jia, M., Optical sensor arrays for the detection and discrimination of natural products. *Nat Prod Rep* **2023**, *40* (3), 628-645.
- (17) Lu, Z.; Lu, N.; Xiao, Y.; Zhang, Y.; Tang, Z.; Zhang, M., Metal-Nanoparticle-Supported Nanozyme-Based Colorimetric Sensor Array for Precise Identification of Proteins and Oral Bacteria. *ACS Appl Mater Interfaces* **2022**, *14* (9), 11156-11166.
- (18) Pu, F.; Ren, J.; Qu, X., Recent progress in sensor arrays using nucleic acid as sensing elements. *Coord Chem Rev* **2022**, *456*, 214379.
- (19) Liu, Z.; Zhu, X.; Lu, Q.; Liu, M.; Li, H.; Zhang, Y.; Liu, Y.; Yao, S., Recognition Engineering-Mediated Multichannel Sensor Array for Gut Microbiota Sensing. *Anal Chem* **2023**, *95* (14), 5911-5919.
- (20) Sun, Z.; Fan, Y. Z.; Du, S. Z.; Yang, Y. Z.; Ling, Y.; Li, N. B.; Luo, H. Q., Conversion of Fluorescence Signals into Optical Fingerprints Realizing High-Throughput Discrimination of Anionic Sulfonate Surfactants with Similar Structure Based on a Statistical Strategy and Luminescent Metal-Organic Frameworks. *Anal Chem* **2020**, *92* (10), 7273-7281.
- (21) Qiao, M.; Cao, Y.; Liu, T.; Ding, L.; Fang, Y., A dual-chromophore-based cross-reactive fluorescent sensor for efficient discrimination of multiple anionic surfactants. *Sensor Actuat B-Chem* **2021**, *331*, 129408.
- (22) Jiang, M.; Yan, X.; Wang, Y.; Pu, F.; Liu, H.; Li, Y.; Yang, C.; Zhu, J.; Liu, X.; Ren, J.; Qu, X., One-Component Artificial Gustatory System Based on Hydrogen-Bond Organic Framework for Discrimination of Versatile Analytes. *Adv Func Mater* **2023**, *33* (24), 2300091.
- (23) Hizir, M. S.; Robertson, N. M.; Balcioglu, M.; Alp, E.; Rana, M.; Yigit, M. V., Universal sensor array for highly selective system identification using two-dimensional nanoparticles. *Chem Sci* **2017**, *8* (8), 5735-5745.
- (24) Wang, J.; Jiang, Z.; Wei, Y.; Wang, W.; Wang, F.; Yang, Y.; Song, H.; Yuan, Q., Multiplexed Identification of Bacterial Biofilm Infections Based on Machine-Learning-Aided Lanthanide Encoding. *ACS Nano* **2022**, *16* (2), 3300-3310.
- (25) Wang, Q.; Liu, Q.; Du, X.-M.; Zhao, B.; Li, Y.; Ruan, W.-J., A white-light-emitting single MOF sensor-based array for berberine homologue discrimination. *J Mater Chem C* **2020**, *8* (4), 1433-1439.
- (26) Long, S.; Qiao, Q.; Deng, F.; Miao, L.; Yoon, J.; Xu, Z., Self-assembling nanoprobe that displays two-dimensional fluorescent signals for identification of surfactants and bacteria. *Chemical Communications* **2019**, *55* (7), 969-972.
- (27) Yang, J.-Y.; Yang, T.; Wang, X.-Y.; Wang, Y.-T.; Liu, M.-X.; Chen, M.-L.; Yu, Y.-L.; Wang, J.-H., A Novel Three-Dimensional Nanosensing Array for the Discrimination of Sulfur-Containing Species and Sulfur Bacteria. *Anal Chem* **2019**, *91* (9), 6012-6018.
- (28) Gao, G.; Chen, J.-H.; Li, C.-J.; Wang, C.-S.; Hu, J.; Zhou, H.; Lin, P.; Xu, Q.; Zhao, W.-W., Duplex-Specific Nuclease-Enabled Target Recycling on Semiconducting Metal-Organic Framework Heterojunctions for Energy-Transfer-Based Organic Photoelectrochemical Transistor miRNA Biosensing. *Anal Chem* **2022**, *94* (45), 15856-15863.
- (29) Wei, D.; Li, M.; Wang, Y.; Zhu, N.; Hu, X.; Zhao, B.; Zhang, Z.; Yin, D., Encapsulating gold nanoclusters into metal-organic frameworks to boost luminescence for sensitive detection of copper ions and organophosphorus pesticides. *J. Hazard. Mater.* **2023**, *441*, 129890.
- (30) Wang, M.; Duan, B.; Li, Y.; Jiang, S.; Huang, Z.; Yang, W., Glutathione-Capped Au Nanoclusters Embedded in NaCl Crystals for White Light-Emitting Devices. *ACS Appl Nano Mater* **2021**, *4* (7), 7486-7492.

- (31) Ma, J.; Lu, Z.; Li, C.; Luo, Y.; Shi, Y. E.; Alam, P.; Lam, J. W. Y.; Wang, Z.; Tang, B. Z., Fluorescence ratiometric assay for discriminating GSH and Cys based on the composites of UiO-66-NH₂ and Cu nanoclusters. *Biosens Bioelectron* **2022**, *215*, 114582.
- (32) Wei, D.; Xiong, D.; Zhu, N.; Wang, Y.; Hu, X.; Zhao, B.; Zhou, J.; Yin, D.; Zhang, Z., Copper Peroxide Nanodots Encapsulated in a Metal-Organic Framework for Self-Supplying Hydrogen Peroxide and Signal Amplification of the Dual-Mode Immunoassay. *Anal Chem* **2022**, *94* (38), 12981-12989.
- (33) Liu, J.; Wang, X.; Zhao, Y.; Xu, Y.; Pan, Y.; Feng, S.; Liu, J.; Huang, X.; Wang, H., NH₃ Plasma Functionalization of UiO-66-NH₂ for Highly Enhanced Selective Fluorescence Detection of U(VI) in Water. *Anal Chem* **2022**, *94* (28), 10091-10100.
- (34) Luo, S.; Gao, J.; Xian, J.; Ouyang, H.; Wang, L.; Fu, Z., Defective Site Modulation Strategy for Preparing Single Atom-Dispersed Catalysts as Superior Chemiluminescent Signal Probes. *Anal Chem* **2022**, *94* (39), 13533-13539.
- (35) Wang, H.; Da, L.; Yang, L.; Chu, S.; Yang, F.; Yu, S.; Jiang, C., Colorimetric fluorescent paper strip with smartphone platform for quantitative detection of cadmium ions in real samples. *J Hazard Mater* **2020**, *392*, 122506.
- (36) Wei, J.-Z.; Gong, F.-X.; Sun, X.-J.; Li, Y.; Zhang, T.; Zhao, X.-J.; Zhang, F.-M., Rapid and Low-Cost Electrochemical Synthesis of UiO-66-NH₂ with Enhanced Fluorescence Detection Performance. *Inorg Chem* **2019**, *58* (10), 6742-6747.
- (37) Wang, N.; Shi, J.; Liu, Y.; sun, W.; Su, X., Constructing bifunctional metal-organic framework based nanozymes with fluorescence and oxidase activity for the dual-channel detection of butyrylcholinesterase. *Anal Chim Acta* **2022**, *1205*.
- (38) Shen, L.; Wu, W.; Liang, R.; Lin, R.; Wu, L., Highly dispersed palladium nanoparticles anchored on UiO-66(NH₂) metal-organic framework as a reusable and dual functional visible-light-driven photocatalyst. *Nanoscale* **2013**, *5* (19), 9374-82.
- (39) Zhu, X.; Li, B.; Yang, J.; Li, Y.; Zhao, W.; Shi, J.; Gu, J., Effective adsorption and enhanced removal of organophosphorus pesticides from aqueous solution by Zr-based MOFs of UiO-67. *ACS Appl Mater Interfaces* **2015**, *7* (1), 223-31.
- (40) Yu, F.; Du, T.; Wang, Y.; Li, C.; Qin, Z.; Jiang, H.; Wang, X., Ratiometric fluorescence sensing of UiO-66-NH₂ toward hypochlorite with novel dual emission in vitro and in vivo. *Sensor Actuat B-Chem* **2022**, *353*, 131032.
- (41) Wei, D.; Wang, Y.; Zhu, N.; Xiao, J.; Li, X.; Xu, T.; Hu, X.; Zhang, Z.; Yin, D., A Lab-in-a-Syringe Device Integrated with a Smartphone Platform: Colorimetric and Fluorescent Dual-Mode Signals for On-Site Detection of Organophosphorus Pesticides. *ACS Appl Mater Interfaces* **2021**, *13* (41), 48643-48652.
- (42) Chen, N.; Wu, S.; Pan, B.; Yang, Z.; Pan, B., Engineering Nano-Au-Based Sensor Arrays for Identification of Multiple Ni(II) Complexes in Water Samples. *Environ Sci Technol* **2023**, *57* (26), 9874-9883.
- (43) Yu, T.; Fu, Y.; He, J.; Zhang, J.; Xianyu, Y., Identification of Antibiotic Resistance in ESKAPE Pathogens through Plasmonic Nanosensors and Machine Learning. *ACS Nano* **2023**, *17* (5), 4551-4563.
- (44) Yang, S.; Sun, J.; Li, X.; Zhou, W.; Wang, Z.; He, P.; Ding, G.; Xie, X.; Kang, Z.; Jiang, M., Large-scale fabrication of heavy doped carbon quantum dots with tunable-photoluminescence and sensitive fluorescence detection. *J Mater Chem A* **2014**, *2* (23), 8660-8667.
- (45) Hammler, D.; Marx, A.; Zumbusch, A., Fluorescence-Lifetime-Sensitive Probes for Monitoring ATP Cleavage. *Chem-Eur J* **2018**, *24* (57), 15329-15335.



Scheme 1. Schematic diagram showing the fabrication of dual-emission single sensing element-assembled fluorescent sensor array and its application for rapid discrimination of multiple surfactants.

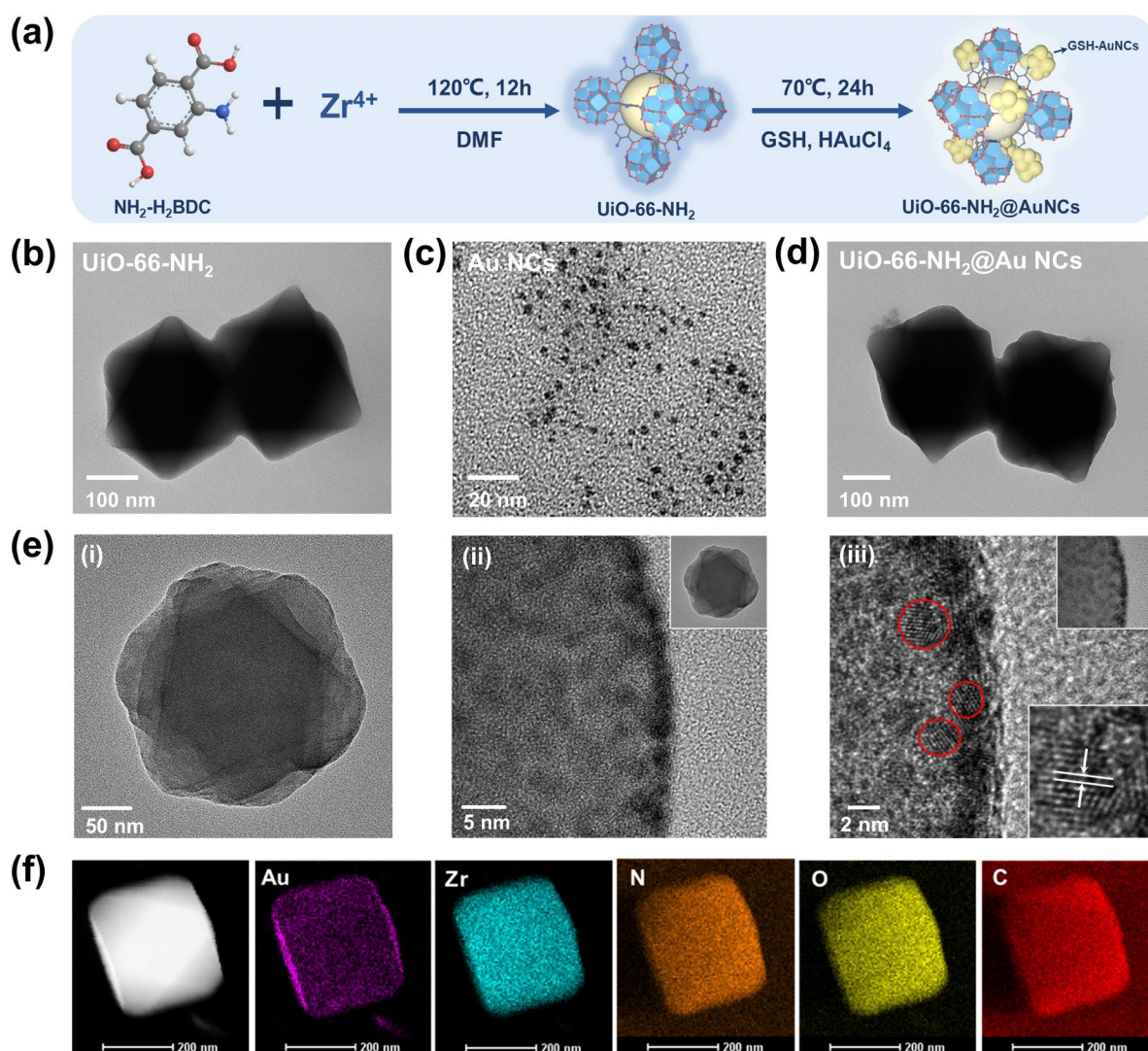


Figure 1. (a) The preparation of UiO-66-NH₂@Au NCs. TEM images of (b) UiO-66-NH₂, (c) Au NCs, and (d) UiO-66-NH₂@Au NCs. (e) High-resolution TEM images of UiO-66-NH₂@Au NCs. (f) Images of dark-field scanning TEM and corresponding EDS elemental mapping (Au, Zr, N, O, and C) of UiO-66-NH₂@Au NCs.

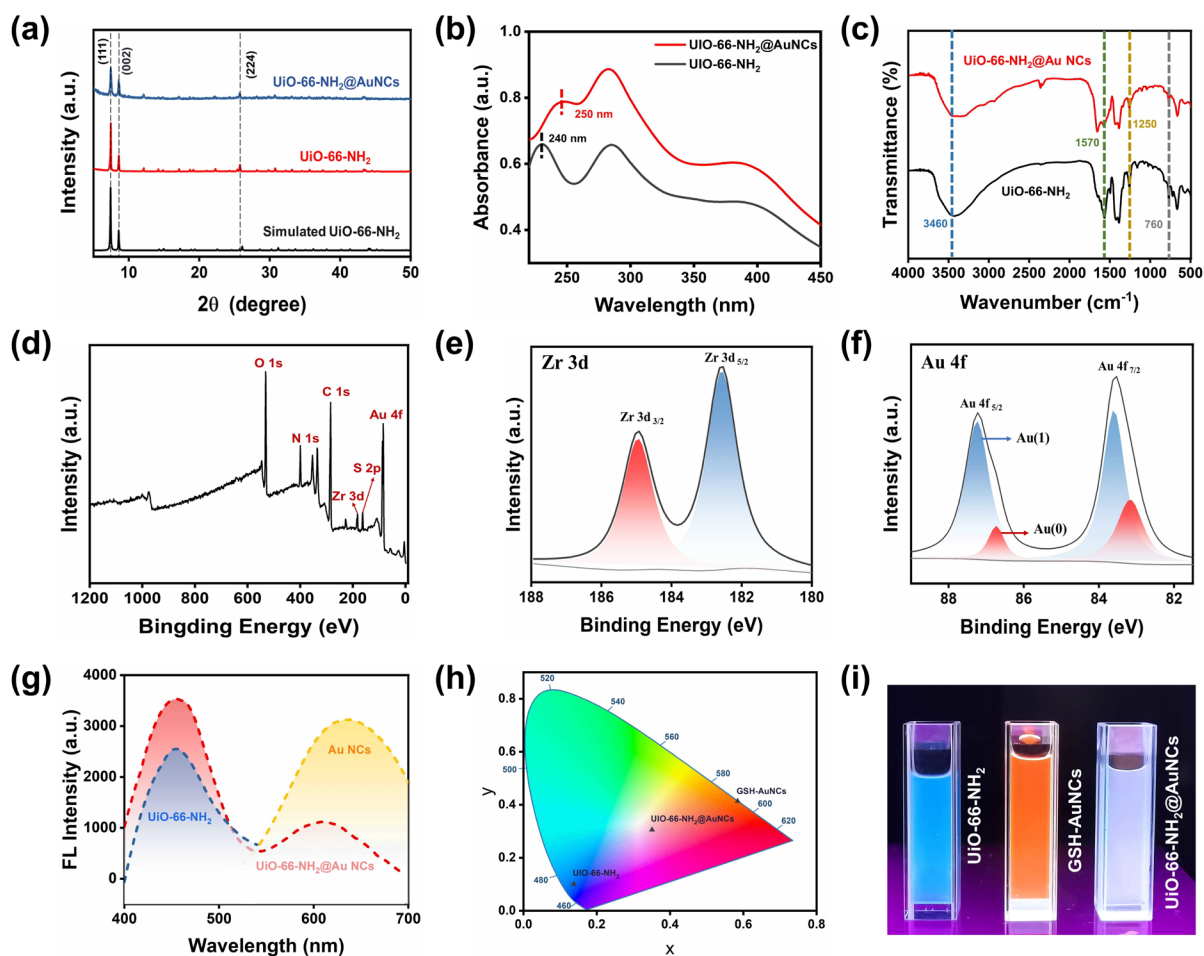


Figure 2. (a) PXRD patterns of UiO-66-NH₂@Au NCs, UiO-66-NH₂, and simulated UiO-66-NH₂. (b) UV-vis absorption spectra of UiO-66-NH₂@Au NCs and UiO-66-NH₂. (c) FTIR spectra of UiO-66-NH₂@Au NCs and UiO-66-NH₂. (d) XPS spectra of UiO-66-NH₂@Au NCs. (e) Zr 3d and (f) Au 4f spectrum of UiO-66-NH₂@Au NCs. (g) Fluorescence spectra of the UiO-66-NH₂, Au NCs, and UiO-66-NH₂@Au NCs. (h) CIE chromaticity diagram for the UiO-66-NH₂, Au NCs, and UiO-66-NH₂@Au NCs. (i) Photographs of UiO-66-NH₂, GSH-Au NCs, and UiO-66-NH₂@Au NCs under UV lamp irradiation.

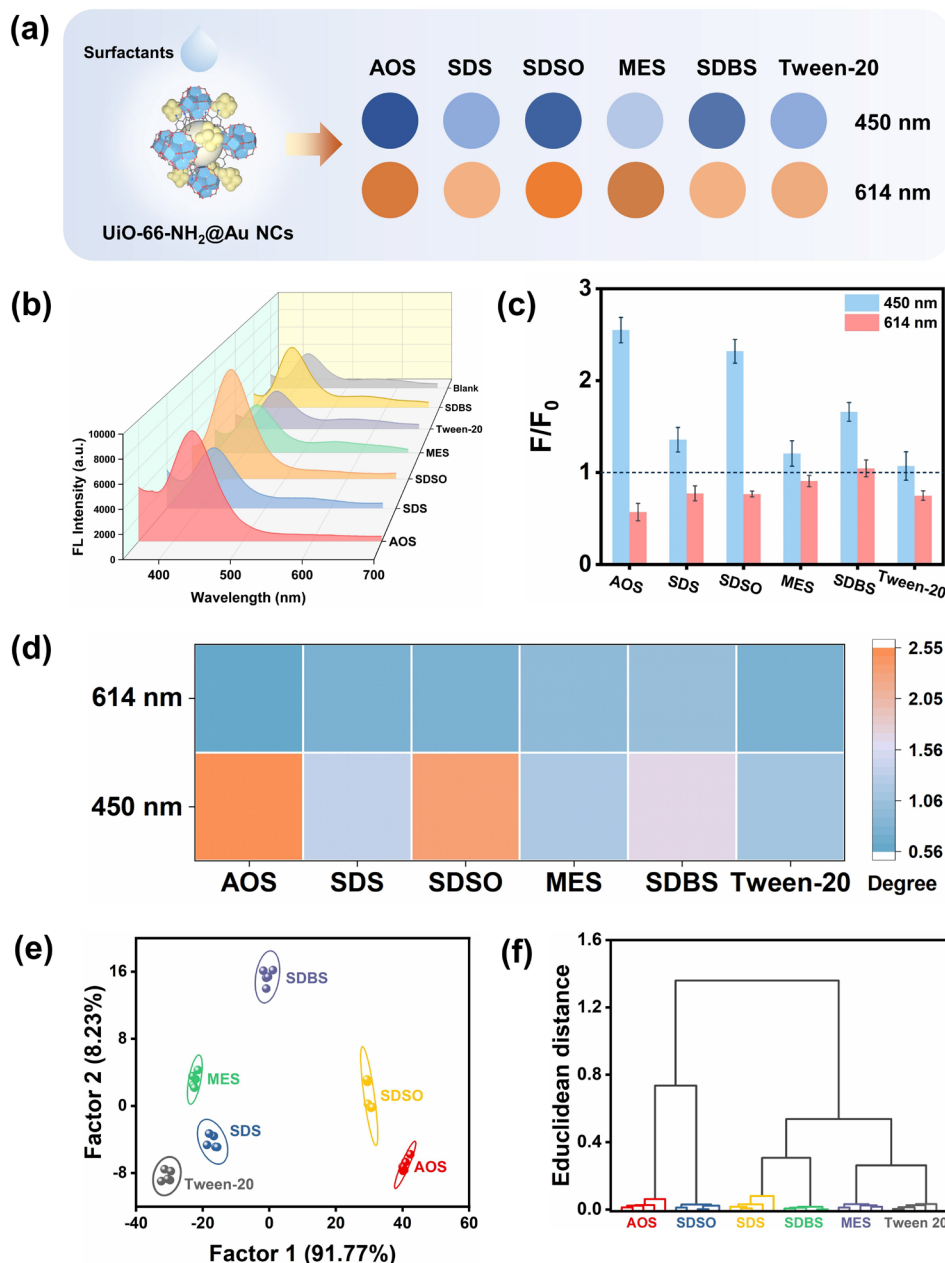


Figure 3. (a) Schematic diagram showing the fluorescence sensor array based on UiO-66-NH₂@Au NCs for six surfactants detection. (b) Fluorescent responses of the UiO-66-NH₂@Au NCs to six surfactants (AOS, SDS, SDSO, MES, SDBS, and Tween-20). (c) Fluorescence intensity ratio (F/F_0) of UiO-66-NH₂@Au NCs at 450 and 614 nm with the addition of six surfactants. (d) Heat map generated from fluorescence patterns of fluorescence sensor array. (e) Linear discriminant analysis (LDA) and (f) hierarchical cluster analysis (HCA) plot for the identification of six surfactants derived from the fluorescence response patterns.

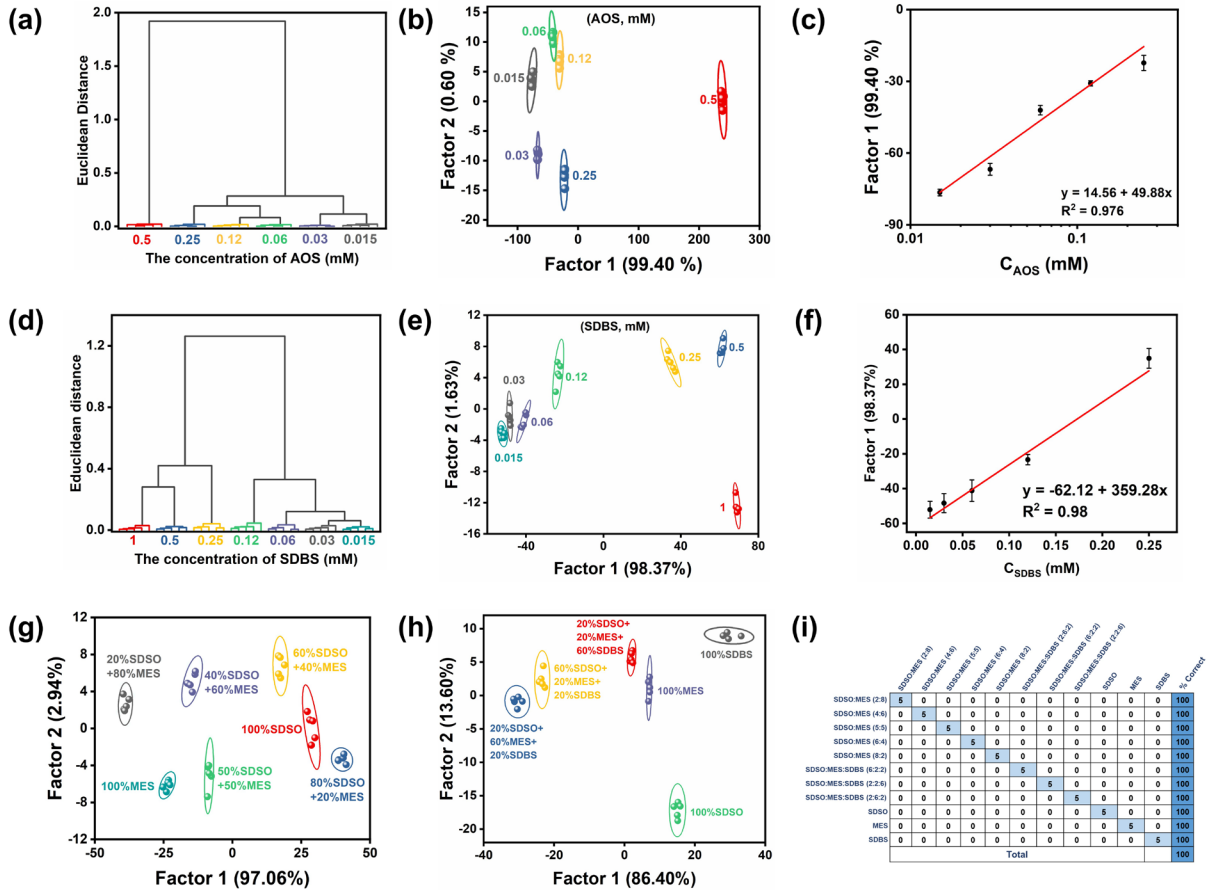


Figure 4. (a, d) HCA and (b, e) LDA plot for fluorescence response patterns toward different concentrations of AOS and SDBS. Linear relationships between Factor 1 and various concentrations of (c) AOS and (f) SDBS. LDA plot for fluorescence response patterns toward (g) the mixtures of pure SDSO, MES, and their mixtures, and (h) pure SDSO, MES, SDBS, and their mixtures. (i) The classified prediction confusion matrix heat map for the discrimination of pure SDSO, MES, SDBS, and their mixtures with five parallel measurements.

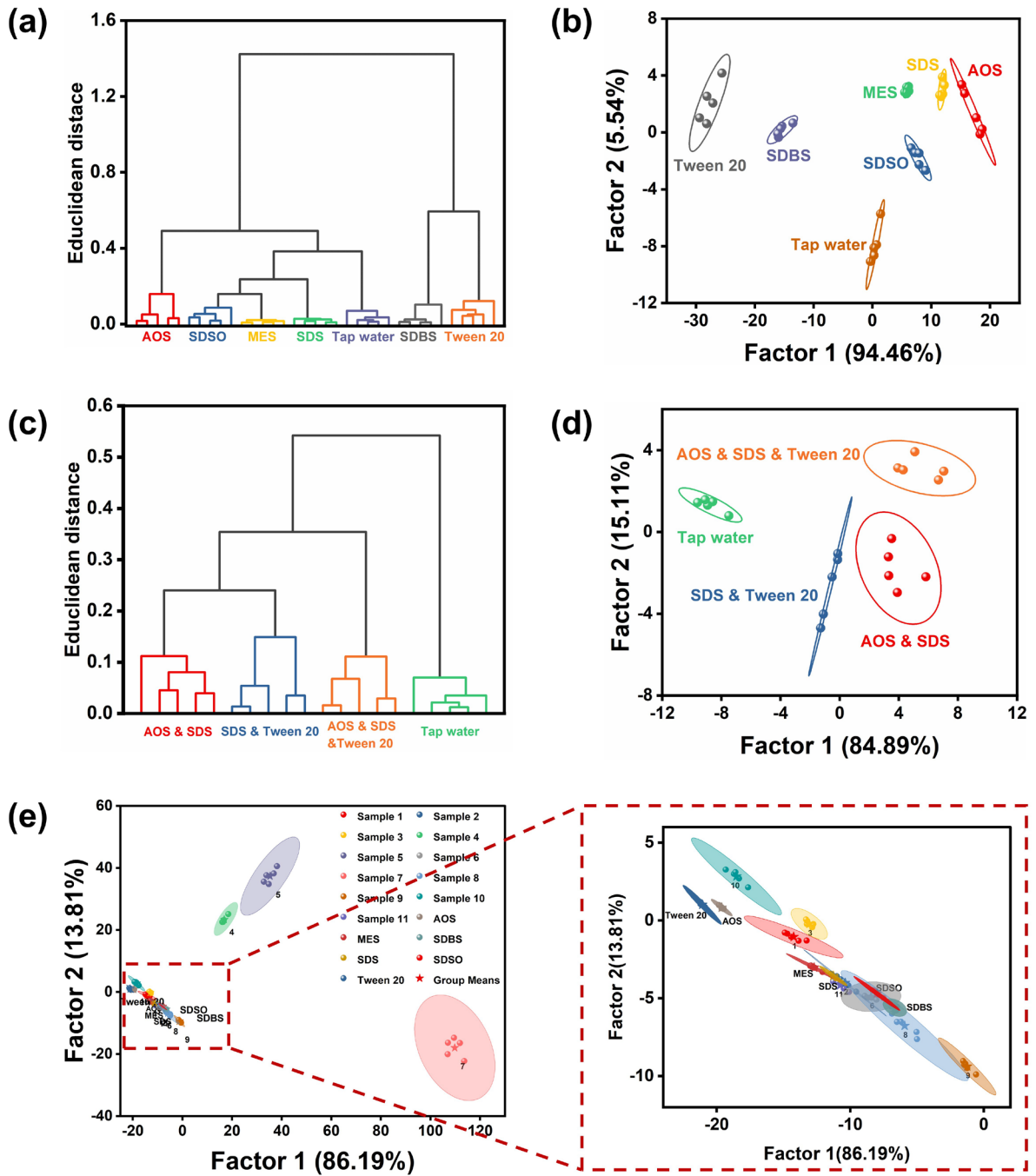
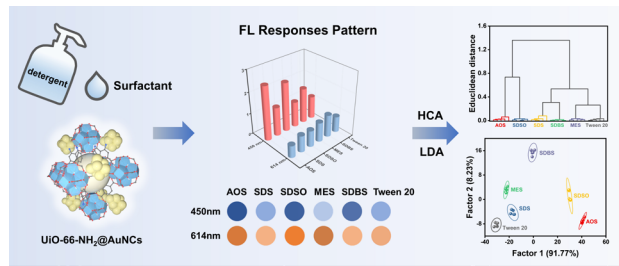


Figure 5. (a) HCA and (b) LDA analysis of different surfactants in tap water samples by the proposed sensor array. (c) HCA and (d) LDA analysis of binary and ternary mixtures of surfactants in tap water samples by the proposed sensor array. (e) LDA plot for discrimination of surfactants in real washing and disinfecting samples.

For Table of Contents Only



Dual-emission single sensing element-assembled fluorescent sensor arrays for the rapid discrimination of multiple surfactants in environments

Wei, Dali

2024-03-26

Attribution 4.0 International

Wei D, Zhang H, Tao Y, et al., (2024) Dual-emission single sensing element-assembled fluorescent sensor arrays for the rapid discrimination of multiple surfactants in environments.

Analytical Chemistry. Volume 96, Issue 12, March 2024, pp. 4987-4996

<https://doi.org/10.1021/acs.analchem.4c00108>

Downloaded from CERES Research Repository, Cranfield University